The ROYAL COLLEGE *of*
OPHTHALMOLOGISTS

ARTICLE

Clinical features of microvasculature in subzones of parapapillary atrophy in myopic eyes: an OCT-angiography study

Xinxin Hu[1,2,4,5] · Kunte Shang[1,2] · Xiaoxiao Chen[1,2] · Xinghuai Sun[1,2,3] · Yi Dai[1,2]

Abstract

Purpose To investigate the microvasculature in subzones of parapapillary atrophy (PPA) and their associated factors in healthy myopic eyes using optical coherence tomography (OCT) angiography.

Methods The cross-sectional study included 55 healthy myopic eyes with PPA. The superficial radial peripapillary capillary (RPC) and choroidal microvascular densities were delineated and measured in alpha, beta, and gamma zone PPA using OCT angiography, respectively. The structural parameters including the width and area in each subzone and corresponding retinal nerve fiber layer thickness were further measured. Statistical analysis was performed to explore the relationship between the vascular and structural parameters.

Results The mean age and mean axial length of the participants were 27.55 ± 5.72 years and 25.19 ± 1.08 mm. Among alpha, beta, and gamma zone PPA, the beta zone showed the lowest RPC density, which was negatively correlated with the area and width of beta zone ($P < 0.05$). The gamma zone showed the highest RPC density, which was positively correlated with the retinal nerve fiber layer thickness of gamma zone ($P < 0.01$). Compared with alpha zone, both gamma and beta zones showed marked decrease of choriocapillaris. The beta zone showed a lower choroidal microvascular density than that of gamma zone ($P < 0.01$). Choroidal microvascular density in beta and gamma zones were negatively correlated with the width of beta zone and gamma zone, respectively ($P < 0.01$).

Conclusions Topographic differences on superficial RPC and choroidal microvasculature were found among the subzones of PPA. A microcirculatory deficiency in beta zone PPA may exist in myopic eyes.

✉ Yi Dai
ydai@fudan.edu.cn

1. Department of Ophthalmology and Visual Science, Eye and ENT Hospital, Shanghai Medical College, Fudan University, Shanghai 200031, China

2. NHC Key Laboratory of Myopia (Fudan University), Key Laboratory of Myopia, Chinese Academy of Medical Sciences, and Shanghai Key Laboratory of Visual Impairment and Restoration, Fudan University, Shanghai 200031, China

3. State Key Laboratory of Medical Neurobiology, Institutes of Brain Science, Collaborative Innovation Center for Brain Science, Fudan University, Shanghai 200032, China

4. Department of Ophthalmology, Yinzhou Hospital Affiliated to Medical School of Ningbo University, Ningbo 315000, China

5. The Eye Hospital of Wenzhou Medical University (Ningbo Branch), Ningbo 315000, China

Introduction

Parapapillary atrophy (PPA) is a common clinical finding surrounding the optic disc. PPA has been conventionally differentiated into an alpha zone and a beta zone based on its appearance on fundus photographs [1]. The alpha zone was defined as irregular hyperpigmentation and hypopigmentation in peripheral area of PPA. The beta zone was defined as visible large choroidal vessels and sclera between the optic disc border and alpha zone. PPA has long been suggested to be associated with glaucoma and myopia [2–5]. However, the mechanism underlying PPA formation and enlargement remains largely unknown.

The classic beta zone PPA has recently been categorized into a new beta zone and a gamma zone based on the location of the termination of peripapillary Bruch's membrane [6, 7]. The gamma zone was defined as the peripapillary area free of Bruch's membrane, and the new beta zone was defined by the continued presence of Bruch´s membrane and absence of retinal pigment epithelium

(RPE). Mainly based on spectral domain OCT findings, the new beta zone PPA was found to be associated with the older age and the presence of glaucoma [7–11], while the gamma zone PPA was strongly correlated with axial myopia and disc rotations around vertical and horizontal axes [12–14].

Recent advances in OCT angiography enable visualization and quantification of perfused vessels in different layers of the retina and choroid in a fast, reliable, and noninvasive way [15, 16]. Several studies have reported the microvascular features of PPA in myopic and glaucomatous eyes using OCT angiography [17–19]. To our knowledge, previous studies addressing PPA-related vessel density used the parameter of average peripapillary microvascular density. Details of microvasculature in subzones of PPA have not been elucidated yet, which may provide more specific and direct evidence regarding the pathogenesis of PPA formation. Therefore, the aim of the present study was to investigate the superficial RPC and deep microvascular densities and their associated factors in alpha, beta and gamma zone PPA of myopic eyes using OCT angiography.

Materials and methods

Study participants

This study included 55 healthy myopic eyes from 55 adult participants from Shanghai Eye & ENT Hospital of Fudan University. All procedures of this study were in accordance with the tenets of the Declaration of Helsinki for research involving human subjects and under protocols approved by the Ethics Committee of the Eye and ENT Hospital of Fudan University, China. Written informed consents were obtained from all participants.

All participants had no known ophthalmic diseases other than myopia as determined by comprehensive ophthalmic examinations. The recruitment criteria included normal eyes, as determined by slit-lamp biomicroscopy, fundus examination and OCT; best-corrected visual acuity of 16/20 or better; and intraocular pressure (IOP) of 21 mmHg or lower. In addition, subjects were required to have a clear delectability of PPA including the three subzones on fundus photographs and/or B-scan OCT images. Exclusion criteria included the following: (1) evidence of glaucoma, diabetic retinopathy, other ocular, or systemic diseases which might affect the ocular circulation; (2) a history of intraocular surgery or ocular injury; (3) current or recent (within 2 weeks of measurements) use of an agent (by any administering method) known to affect visual function; (4) an anterior segment disorder or media opacity that affected image quality. One eye of each participant was randomly selected if both eyes have PPA.

Axial length and central corneal thickness were measured by Lenstar (LS 900; Haag-Streit Diagnostics, USA). IOP (Auto Tonometer TX-F; Topcon, Tokyo, Japan), pulse rate, systolic and diastolic blood pressure (BP) were recorded within 5 min after the OCT imaging. The mean arterial pressure (MAP) and the ocular perfusion pressure (OPP) were determined by the formula: $MAP = DBP + 0.42 (SBP - DBP)$ and $OPP = 2/3 MAP - IOP$ [20, 21].

OCT angiography scanning of the peripapillary area

OCT angiography, a spectral domain OCT (RTVue-XR Avanti; Optovue, Fremont, CA, USA), was obtained to image the peripapillary areas. To identify perfused vessels, the volumetric scans were processed by the SSADA algorithm. For each area, four volumetric raster scans, including two in the horizontal priority (x-fast) and two in the vertical priority (y-fast), were taken consecutively. After scan acquisition, an orthogonal registration algorithm was used to remove the motion artifacts and to merge the two-dimensional scans into 3D OCT angiograms. In the current study, images with significant motion artifact, segmentation error, or signal strength index <60 were excluded. One eye of each participant was examined and scanned twice during the same visit.

The scans were acquired over a 4.5×4.5 mm region centered at the optic nerve head. Optic disc and peripapillary regions were automatically segmented by the Angio-Vue disc mode. In order to measure the density of superficial peripapillary microvascular, the software automatically identified the projection signal from the internal limiting membrane to the retinal nerve fiber layer (RNFL) to generate the RPC segment. Vessel density (%) was defined as the proportion of measured area occupied by flowing blood vessels in a particular region. After reviewing the accuracy of the optic disc margin automatically fitted by the software, the line was adjusted manually. Average peripapillary vessel density was calculated in the region defined as a 700-μm-wide elliptical annulus extending outward from the optic disc boundary on the RPC segment. In addition, all participants underwent peripapillary RNFL thickness measurements by Avanti spectral domain OCT using the traditional ONH scans.

Analyses of microvascular density in subzones of PPA

Based on B-scan OCT images and near-infrared reflectance images, the alpha zone PPA was defined as Bruch membrane with irregular RPE. The beta zone PPA was defined as the presence of Bruch's membrane without the RPE, while the gamma zone PPA was characterized by the absence of Bruch's membrane as previously described [7].

Table 1 Summary of demographic and clinical characteristics of participants.

Characteristics	Mean ± SD (range)	Correlation with superficial peripapillary vessel density (P value)
Peripapillary RPC density (%)	61.80 ± 3.59 (45.46–67.44)	–
Gender (male: female)	20:35	0.068
Age (years)	27.55 ± 5.72 (22–49)	0.55
IOP (mmHg)	15.53 ± 1.98 (11.9–20.3)	0.15
Axial length (mm)	25.19 ± 1.08 (23.09–27.99)	0.002
DBP (mmHg)	68.73 ± 8.33 (53–89)	0.25
SBP (mmHg)	111.96 ± 11.10 (90–147)	0.39
BP amplitude (mmHg)	43.24 ± 9.78 (27–71)	0.99
MAP (mmHg)	86.89 ± 8.28 (71.96–105.82)	0.25
OPP (mmHg)	42.39 ± 5.62 (30.26–55.35)	0.53
Pulse rate (bpm)	76.29 ± 9.67 (60–99)	0.67
Peripapillary RNFL thickness (μm)	100.89 ± 8.03 (84–118)	0.002

IOP intraocular pressure, *DBP* diastolic blood pressure, *SBP* systolic blood pressure, *BP* blood pressure, *MAP* mean arterial pressure, *OPP* mean ocular perfusion pressure, *RNFL* retinal nerve fibre layer.

After acquiring both en face and angiographic images of the optic disc at the same position, the boundaries of the optic disc, alpha zones, beta zone, and gamma zone PPA were delineated on en face images according to the serial B-scan images. The area and flow at the level of RPC in delineated regions will be automatically reported by the built-in software of RTVue-XR Avanti. The RPC density (%) of selected subzones was calculated as the RPC flow divided by area. We checked the automatic retinal segmentation and manually adjusted the segmentation lines of RNFL in the parapapillary gamma zone and beta zone if necessary. The choroid microvascular density in beta zone and gamma zone PPA was measured as previously described [22]. Briefly, the large peripapillary vessels at the angiographic images of choroid level were delineated and excluded from further measurements. Beta zone and gamma zone PPA were divided by the delineated large peripapillary vessels into several small regions. The choroidal microvascular density in each small region was calculated and then averaged as the choroidal microvascular density in beta zone and gamma zone PPA, respectively.

Simultaneous visualization of B-scan images and en face images were used in order to calculate the RNFL thickness of alpha zone, beta zone, and gamma zone PPA. The average RNFL thickness of the alpha zone, beta zone, and gamma zone PPA were calculated as the corresponding area divided by the width, respectively.

Measurements of the RPC density, choroidal microvascular density, RNFL thickness, the area, and the width of the alpha zone, beta zone, and gamma zone PPA were made by two independent examiners (XH and KS). Averaged data were used in the final analysis.

Statistical analysis

All statistical analyses were performed using SPSS version 22.0 (SPSS, Chicago, IL, USA). Data were expressed as mean ± standard deviation. The one-way analysis of variance (ANOVA) and the Bonferroni-*t* test were used to compare the differences among alpha zone, beta zone, and gamma zone PPA. Linear regression analyses were performed to analyse the effects of other independent parameters on the RPC density and choroidal microvascular density. All *P* values were two-sided and considered statistically significant when they were less than 0.05 in this study.

Results

The study included 55 normal myopic eyes from 55 subjects. Mean age was 27.55 ± 5.72 years (median, 26 years; range, 22–49 years). Mean axial length was 25.19 ± 1.08 mm (median, 25.32 mm; range, 23.09–27.99 mm). The demographic and clinical characteristics of participants were summarized in Table 1.

Superficial RPC in alpha zone, beta zone, and gamma zone of PPA

Significant differences were observed in RPC density among the alpha zone, beta zone, and gamma zone PPA (Fig. 1). The RPC density of the alpha zone, beta zone, and gamma zone PPA were 59.19 ± 2.98%, 55.85 ± 3.31%, and 63.01 ± 3.83%, respectively (Fig. 2a). The gamma zone PPA showed a highest RPC density, and the beta zone PPA

Fig. 1 Representative images of defining RPC and choroidal microvasculature in subzones of parapapillary atrophy. After acquiring en face (**a**), fundus photograph (**b**), and angiographic (**e, f**) images of the optic disc at the same position, the boundaries of the alpha zone (between blue and purple line/arrow), beta zone (between purple and yellow line/arrow), and gamma zone (between yellow and red line/arrow) were delineated on en face image (**a**) according to the serial B-scan images (**c, d**).
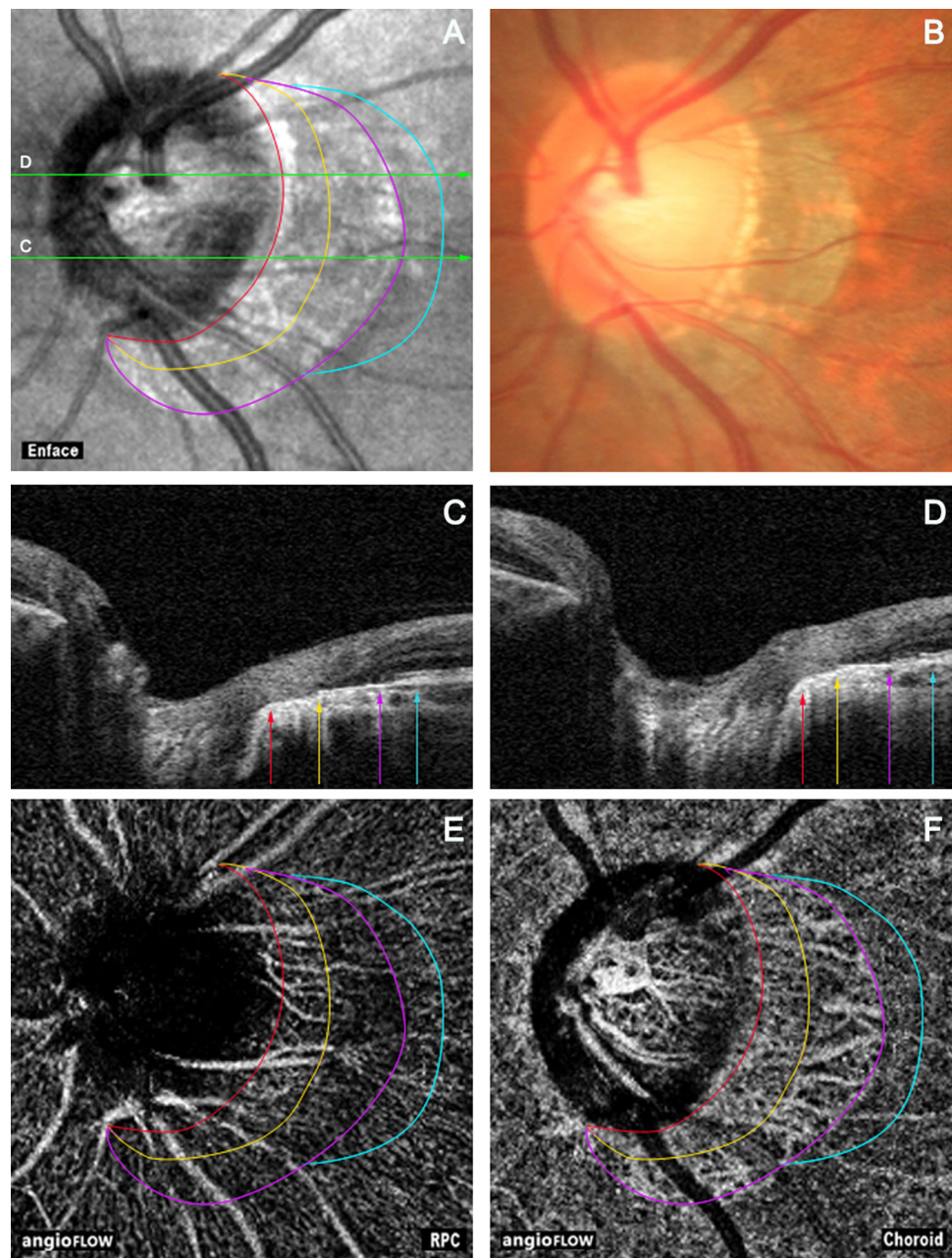

showed the lowest RPC density among three subzones ($P < 0.001$). The RPC density of beta zone PPA was negatively correlated with the area ($P = 0.011$) and the width ($P = 0.023$) of beta zone PPA (Fig. 2c, d). The RPC density of gamma zone PPA was negatively correlated with the width ($P = 0.049$) of gamma zone PPA. The RPC density in alpha zone, beta zone, and gamma zone PPA were not correlated with the axial length, respectively ($P > 0.05$).

Significant difference were also observed in the average RNFL thickness among the alpha zone, beta zone, and gamma zone PPA ($84.12 \pm 11.04 \, \mu m$, $95.87 \pm 10.62 \, \mu m$ and $247.42 \pm 31.69 \, \mu m$ in the alpha zone, beta zone and gamma

zone PPA, respectively). The gamma zone PPA had a thickest average RNFL thickness among three subzones ($P < 0.001$, Fig. 2b). The RPC density of gamma zone PPA was positively correlated with the corresponding RNFL thickness in gamma zone ($P = 0.001$). The RPC density of alpha zone and beta zone PPA were not correlated with the corresponding RNFL thickness in alpha zone and beta zone PPA, respectively ($P > 0.05$, Table 2).

In addition, we analysed the factors associated with average peripapillary RPC density, which was calculated in the peripapillary area defined as a 700-μm-wide elliptical annulus extending outward from the optic disc border on the

Fig. 2 Graphs showing the relationships among major parameters. Box plots showing the comparison of radial peripapillary capillary (RPC) density (**a**) and average retinal nerve fibre layer (RNFL) thickness (**b**) among the alpha zone, beta zone, and gamma zone parapapillary atrophy. Scatterplots show the correlations between the width (**c**), area (**d**) of beta zone, and the RPC of beta zone. Scatterplots also show the correlations between the width (**e**), area (**f**) of the beta zone, and the choroidal microvascular density of the beta zone. **$P < 0.01$, ***$P < 0.001$.
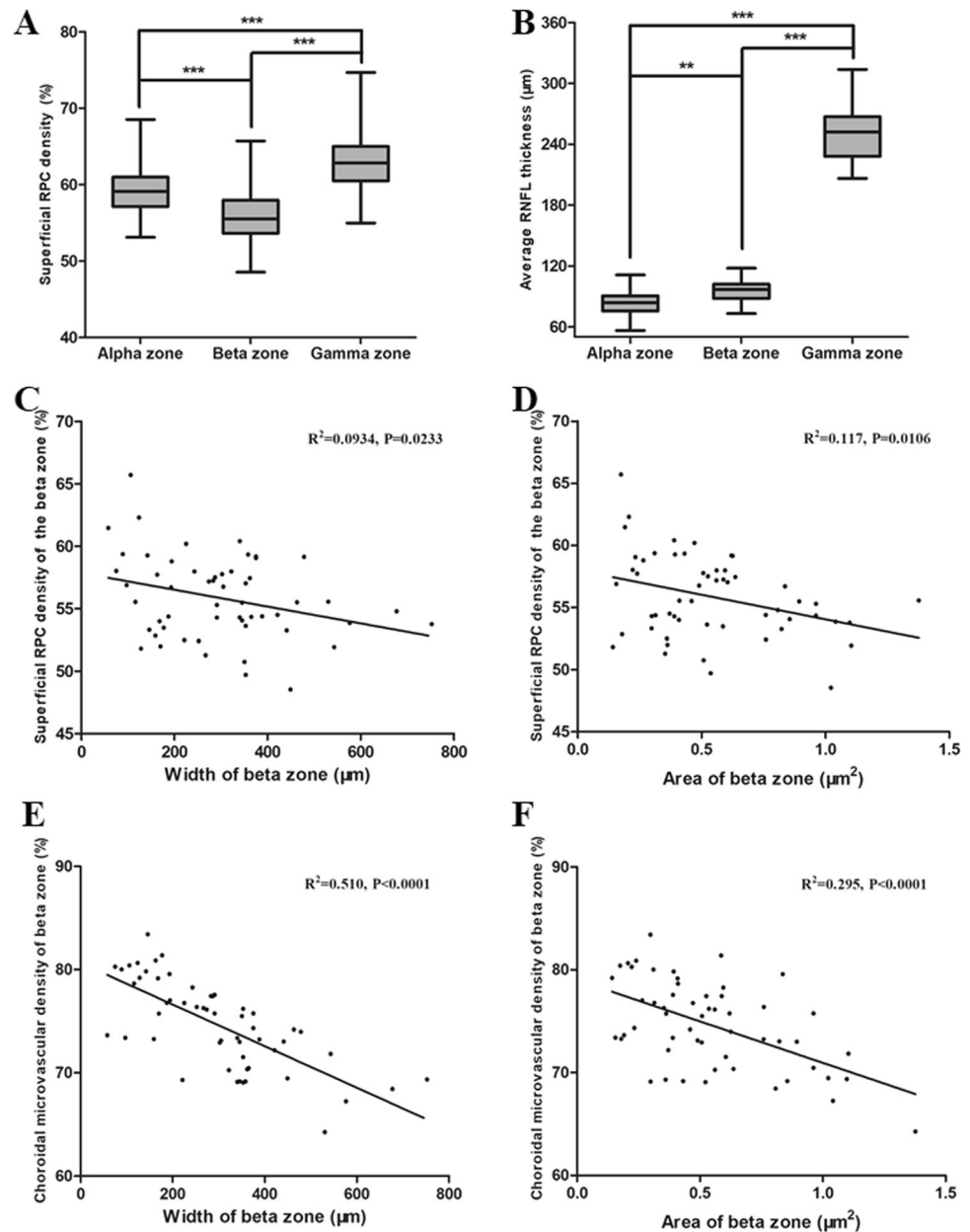
RPC segment. The correlation analysis showed that the average peripapillary RPC density was positively correlated with the average circumpapillary RNFL thickness ($P = 0.002$) and negatively correlated with the axial length ($P = 0.002$, Table 1).

Choroidal microvasculature in alpha zone, beta zone, and gamma zone of PPA

There were topographic correlations between the choriocapillaris patterns and the microstructure of PPA (Fig. 1). The alpha zone PPA showed the relatively normal appearance of choriocapillaris, which was similar to perimacular

area. The beta and gamma zone PPA, however, showed marked decrease of choriocapillaris.

We further measured and compared the choroidal microvascular density in beta and gamma zone PPA. The choroidal microvascular density of the beta zone and gamma zone PPA was $74.65 \pm 4.24\%$, and $82.53 \pm 5.56\%$, respectively ($P = 0.024$). Choroidal microvascular density of beta zone PPA was negatively correlated with the area ($P < 0.001$) and the width ($P < 0.001$, Fig. 2e, f) of beta zone PPA. Choroidal peripapillary microvascular density of gamma zone PPA was negatively correlated with the width ($P = 0.003$) of gamma zone PPA, but not correlated with the area ($P = 0.092$) of gamma zone PPA (Table 3).

Table 2 Correlation with RPC density in alpha zone, beta zone, and gamma zone PPA.

Parameters	Alpha zone		Beta zone		Gamma zone	
	r	P value	r	P value	r	P value
Age (years)	−0.22	0.11	0.052	0.70	0.076	0.58
IOP (mmHg)	0.15	0.26	0.12	0.38	0.027	0.85
OPP (mmHg)	−0.14	0.31	−0.039	0.78	0.011	0.94
Axial length (mm)	−0.26	0.059	−0.26	0.058	−0.12	0.37
Cornea thickness (μm)	−0.057	0.70	−0.013	0.93	−0.13	0.37
Aqueous depth (mm)	−0.069	0.66	−0.23	0.14	−0.11	0.48
Lens thickness (mm)	−0.011	0.95	0.15	0.37	0.077	0.64
Corresponding subzone area (μm^2)	−0.25	0.068	−0.34	0.011	−0.15	0.28
Corresponding subzone width (μm)	−0.22	0.11	−0.31	0.023	−0.27	0.049
Corresponding RNFL thickness (μm)	−0.063	0.65	−0.029	0.83	0.52	<0.001

IOP intraocular pressure, *OPP* mean ocular perfusion pressure.

Table 3 Correlation with choroidal microvascular in beta zone and gamma zone PPA.

Parameters	Beta zone		Gamma zone	
	r	P value	r	P value
Age (years)	0.064	0.64	0.035	0.80
IOP (mmHg)	0.093	0.50	−0.078	0.57
OPP (mmHg)	0.003	0.98	0.016	0.91
Axial length (mm)	−0.21	0.12	−0.14	0.29
Cornea thickness (μm)	0.014	0.93	−0.18	0.24
Aqueous depth (mm)	−0.22	0.16	0.090	0.56
Lens thickness (mm)	0.22	0.18	0.030	0.85
Corresponding subzone area (μm^2)	−0.54	<0.001	−0.23	0.092
Corresponding subzone width (μm)	−0.71	<0.001	−0.40	0.003

IOP intraocular pressure, *OPP* mean ocular perfusion pressure.

Discussion

In the current study, we divided PPA into alpha, beta, and gamma zone PPA based on spectral domain OCT findings [7]. The superficial RPC and choroidal microvascular density in each subzone of PPA was delineated and measured according to the microstructure of PPA. Our data demonstrated that topographic differences on superficial RPC and choroidal microvasculature were found in the subzones of PPA using OCT angiography. The beta zone PPA showed the lowest superficial RPC and choroidal microvascular densities among the three subzones. The gamma zone PPA showed a higher superficial RPC density and a relatively decreased choroidal microvascular density, while the alpha zone PPA showed similar superficial RPC and choroidal microvasculature compared with perimacular area.

The alpha zone PPA was defined as irregular hypopigmentation and hyperpigmentation and found to be occurred in almost all eyes [23]. In this study, the superficial RPC density was 59.19 ± 2.98% in alpha zone PPA, which was higher than the reported superficial vessel density (54.55 ± 2.49%) in nasal side of the perifovea in emmetropic eyes [24]. The RPC density was positively correlated with the RNFL thickness, both of which decreased significantly with increasing distance from the temporal side of the optic disc to the nasal side of the perifovea [25, 26]. The microvasculature within the peripapillary superficial and deep layers are perfused differently by the central retinal artery and short posterior ciliary artery, respectively [27, 28]. The choroid, outer, and middle retinal layers are nourished by branches of the short posterior ciliary arteries, which also supply choroidal optic nerve head structures via an arterial Circle of Zinn–Haller. The RPE appears to be a key entity influencing the loss of choriocapillaris in age-related macular degeneration [29, 30]. The alpha zone PPA has RPE layer, while both the beta and gamma zone PPA not [7]. This could explain the current findings that the alpha zone PPA showed the normal appearance of choriocapillaris similar to perimacular area, while both the beta and gamma zone PPA showed marked decrease of choriocapillaris. Our findings on the microvascular features of alpha zone PPA support the previous notion that no pathogenic role was observed to be related with the presence of alpha zone PPA.

The formation and development of gamma zone PPA are characteristics of axial myopia [31]. A recent longitudinal study reported the formation and enlargement of gamma zone composed by externally oblique border tissue during juvenile myopia progression [32]. Our data showed that among the three subzones of PPA in myopic eyes, the gamma zone had a highest RPC density, which was associated with the thickness of gamma zone RNFL, while it had a relatively decreased choroidal microvascular density, which was negatively associated with the width of gamma zone. Since the microstructure of gamma zone PPA is

composed initially by oblique border tissue at the level of absent Bruch membrane [32], the choroid structure underlying the gamma zone appears to be different from its original condition without gamma zone formation. One may speculate that without the presence of RPE and Bruch membrane and the deep retina layer, the choriocapillaris in gamma zone PPA would disappear first then followed by gradual decrease in deep choroidal circulation. Our findings on the microvascular features of gamma zone PPA suggest that gamma zone may not be a tissue related with atrophy initially. With the enlargement of gamma zone during axial elongation, however, the microcirculation at the choroidal level may decrease in gamma zone PPA.

The microstructural characteristic of beta zone PPA is absence of RPE with continued presence of Bruch membrane [7]. Our data showed that the beta zone had a lowest superficial RPC density among the three subzones of PPA in myopic eyes, which was negatively associated with the size of beta zone. Beta zone PPA also showed a lower choroidal microvascular density than that of gamma zone PPA, which was negatively associated with the size of beta zone PPA. Sung et al. recently reported that the PPA + BM (defined as beta zone PPA in this study) only group had a lower peripapillary superficial RPC and deep vessel density, which were closely correlated with PPA + BM width in young myopic eyes [17]. Their findings are in general agreement with our data, suggesting a microcirculatory deficiency may exist in the beta zone PPA of axial myopia.

The beta zone PPA has been related with age and the presence of glaucoma [7–10]. But the mechanism on beta zone formation and enlargement remains elusive. Lee et al. reported that juxtapapillary choroidal thickness was negatively correlated with the width of beta zone PPA, but not the width of gamma zone PPA, suggesting that the formation of beta zone and juxtapapillary choroidal atrophy may share a common pathogenic mechanism in glaucoma [33]. The choroidal thickness is a measurement of choroidal microstructure, which may not truly reflect the vascular conditions. Our data provide direct evidence that the decreased choroid microcirculation may play a role in the development of beta zone PPA. With regard to superficial retina microvasculature, previous studies have demonstrated that a strong correlation exists between RPC density and RNFL thickness [34–36]. Lee et al. reported that decreased retinal microvasculature was present at the region of RNFL defect in POAG patients, suggesting that the decreased superficial RPC is the secondary loss at the area of glaucomatous RNFL atrophy [37]. However, our data showed that the RPC density in beta zone was the lowest among the three subzones, and it was not correlated with the RNFL thickness in beta zone. It provides evidence that other than the RNFL thickness, other factor may influence the RPC density. The RPCs anatomose with the outer capillary

network, which runs from the inner plexiform layer to the outer plexiform layer [38]. It is possible that with the gradual thinning of deep retina layer due to RPE loss in beta zone PPA, the oxygen demand from the RPC decreased in turn, leading to the decreased microvascular density in beta zone PPA. On the other hand, the oxygen from the choroid circulation could reach the inner plexiform layer [39]. One may discuss that the decreased choroid microcirculation in the beta zone PPA may have an impact on the superficial microcirculation.

The decreased superficial RPC and choroidal microvasculature found in beta zone PPA might explain the frequent development of beta zone PPA in aged and glaucomatous eyes. It is plausible that the choroidal microvascular density in beta zone PPA may decrease first due to the close relationship between RPE and choroid circulation. Reduced choroidal microvascular densities might accelerate the RPE degeneration, which led to the formation of beta zone PPA. Reduced RPC density in parapapillary beta zone may further increase its susceptibility to glaucomatous optic neuropathy.

Potential limitations and strengths of our study should be mentioned. First, it was a cross-sectional study. We were not able to perceive the longitudinal changes on the microvasculature during the formation and enlargement of parapapillary beta and gamma zones. Second, our study did not include glaucomatous eyes so that the clinical significance of reduced microvascular density in parapapillary beta zone had not been fully explored. Further investigations on the relationship between the microcirculation and microstructure of beta zone PPA in myopia and glaucoma are warranted. On the other hand, the methods used in this study and the detailed results regarding the microvasculature in subzones of PPA may provide a deeper insight into the pathogenesis of PPA.

In conclusion, our findings demonstrated that topographic differences on superficial RPC and choroidal microvasculature were found among the subzones of PPA. A microcirculatory deficiency in beta zone PPA may exist in myopic eyes. Further studies will be needed to address the mechanism on the microvascular change in parapapillary beta and gamma zones and their roles in the progression of glaucomatous optic neuropathy.

Summary

What was known before

- Beta zone parapapillary atrophy was associated with the age and glaucoma, while gamma zone parapapillary atrophy was mainly related with axial myopia. A lower peripapillary RPC and choroidal microvascular density were present in myopic eyes.

What this study adds

- Topographic differences on superficial RPC and choroidal microvasculature were found among the subzones of parapapillary atrophy. The beta zone parapapillary atrophy showed the lowest RPC and choroidal microvascular density, suggesting a microcirculatory deficiency in beta zone atrophy may exist in myopic eyes.

Compliance with ethical standards

Conflict of interest The authors declare that they have no conflict of interest.

Publisher's note Springer Nature remains neutral with regard to jurisdictional claims in published maps and institutional affiliations.

References

1. Jonas JB, Nguyen XN, Gusek GC, Naumann GO. Parapapillary chorioretinal atrophy in normal and glaucoma eyes. I. Morphometric data. Invest Ophthalmol Vis Sci. 1989;30:908–18.
2. Jonas JB. Clinical implications of peripapillary atrophy in glaucoma. Curr Opin Ophthalmol. 2005;16:84–8.
3. Manalastas P, Belghith A, Weinreb RN, Jonas JB, Suh MH, Yarmohammadi A, et al. Automated beta zone parapapillary area measurement to differentiate between healthy and glaucoma eyes. Am J Ophthalmol. 2018;191:140–8.
4. Teng CC, De Moraes CG, Prata TS, Liebmann CA, Tello C, Ritch R, et al. The region of largest beta-zone parapapillary atrophy area predicts the location of most rapid visual field progression. Ophthalmology. 2011;118:2409–13.
5. Araie M, Sekine M, Suzuki Y, Koseki N. Factors contributing to the progression of visual field damage in eyes with normal-tension glaucoma. Ophthalmology. 1994;101:1440–4.
6. Jonas JB, Jonas SB, Jonas RA, Holbach L, Dai Y, Sun X, et al. Parapapillary atrophy: histological gamma zone and delta zone. Plos One. 2012;7:e47237.
7. Dai Y, Jonas JB, Huang H, Wang M, Sun X. Microstructure of parapapillary atrophy: beta zone and gamma zone. Investig Ophthalmol Vis Sci. 2013;54:2013–8.
8. Kim YW, Lee EJ, Kim TW, Kim M, Kim H. Microstructure of beta-zone parapapillary atrophy and rate of retinal nerve fiber layer thinning in primary open-angle glaucoma. Ophthalmology. 2014;121:1341–9.
9. Yamada H, Akagi T, Nakanishi H, Ikeda HO, Kimura Y, Suda K, et al. Microstructure of peripapillary atrophy and subsequent visual field progression in treated primary open-angle glaucoma. Ophthalmology. 2016;123:542–51.
10. Yoo YJ, Lee EJ, Kim TW. Intereye difference in the microstructure of parapapillary atrophy in unilateral primary open-angle glaucoma. Investig Ophthalmol Vis Sci. 2016;57:4187–93.
11. Shang K, Hu X, Dai Y. Morphological features of parapapillary beta zone and gamma zone in chronic primary angle-closure glaucoma. Eye. 2019;33:1378–86.
12. Kim M, Kim TW, Weinreb RN, Lee EJ. Differentiation of parapapillary atrophy using spectral-domain optical coherence tomography. Ophthalmology. 2013;120:1790–7.
13. Jonas JB, Wang YX, Zhang Q, Fan YY, Xu L, Wei WB, et al. Parapapillary gamma zone and axial elongation-associated optic disc rotation: the Beijing Eye Study. Investig Ophthalmol Vis Sci. 2016;57:396–402.
14. Zhang Q, Wang YX, Wei WB, Xu L, Jonas JB. Parapapillary beta zone and gamma zone in a healthy population: the Beijing Eye Study 2011. InvestigOphthalmol Vis Sci. 2018;59:3320–9.
15. Spaide RF, Klancnik JJ, Cooney MJ. Retinal vascular layers imaged by fluorescein angiography and optical coherence tomography angiography. JAMA Ophthalmol. 2015;133:45–50.
16. Wang X, Jiang C, Ko T, Kong X, Yu X, Min W, et al. Correlation between optic disc perfusion and glaucomatous severity in patients with open-angle glaucoma: an optical coherence tomography angiography study. Graefes Arch Clin Exp Ophthalmol. 2015;253:1557–64.
17. Sung MS, Heo H, Park SW. Microstructure of parapapillary atrophy is associated with parapapillary microvasculature in myopic eyes. Am J Ophthalmol. 2018;192:157–68.
18. Akagi T, Iida Y, Nakanishi H, Terada N, Morooka S, Yamada H, et al. Microvascular density in glaucomatous eyes with hemifield visual field defects: an optical coherence tomography angiography study. Am J Ophthalmol. 2016;168:237–49.
19. Sakaguchi K, Higashide T, Udagawa S, Ohkubo S, Sugiyama K. Comparison of sectoral structure-function relationships in glaucoma: vessel density versus thickness in the peripapillary retinal nerve fiber layer. Investig Ophthalmol Vis Sci. 2017;58:5251–62.
20. Longo A, Geiser MH, Riva CE. Posture changes and subfoveal choroidal blood flow. Investig Ophthalmol Vis Sci. 2004;45:546–51.
21. Riva CE, Grunwald JE, Petrig BL. Autoregulation of human retinal blood flow. an investigation with laser Doppler velocimetry. Investig Ophthalmol Vis Sci. 1986;27:1706–12.
22. Sung MS, Lee TH, Heo H, Park SW. Clinical features of superficial and deep peripapillary microvascular density in healthy myopic eyes. Plos One. 2017;12:e187160.
23. Kubota T, Jonas JB, Naumann GO. Direct clinico-histological correlation of parapapillary chorioretinal atrophy. Br J Ophthalmol. 1993;77:103–6.
24. Guo Y, Sung MS, Park SW. Assessment of superficial retinal microvascular density in healthy myopia. Int Ophthalmol. 2019;39:1861–70.
25. Mase T, Ishibazawa A, Nagaoka T, Yokota H, Yoshida A. Radial peripapillary capillary network visualized using wide-field montage optical coherence tomography angiography. Investig Ophthalmol Vis Sci. 2016;57:T504–T510.
26. Mansoori T, Sivaswamy J, Gamalapati JS, Balakrishna N. Topography and correlation of radial peripapillary capillary density network with retinal nerve fibre layer thickness. Int Ophthalmol. 2018;38:967–74.
27. Lieberman MF, Maumenee AE, Green WR. Histologic studies of the vasculature of the anterior optic nerve. Am J Ophthalmol. 1976;82:405–23.
28. Onda E, Cioffi GA, Bacon DR, Van Buskirk EM. Microvasculature of the human optic nerve. Am J Ophthalmol. 1995;120:92–102.
29. McLeod DS, Grebe R, Bhutto I, Merges C, Baba T, Lutty GA. Relationship between RPE and choriocapillaris in age-related

macular degeneration. Investig Ophthalmol Vis Sci. 2009;50: 4982–91.

30. Korte GE, Reppucci V, Henkind P. RPE destruction causes choriocapillary atrophy. Investig Ophthalmol Vis Sci. 1984;25: 1135–45.

31. Kim TW, Kim M, Weinreb RN, Woo SJ, Park KH, Hwang JM. Optic disc change with incipient myopia of childhood. Ophthalmology. 2012;119:21–6.

32. Kim M, Choung HK, Lee KM, Oh S, Kim SH. Longitudinal changes of optic nerve head and peripapillary structure during childhood myopia progression on OCT: Boramae Myopia Cohort Study Report 1. Ophthalmology. 2018;125: 1215–23.

33. Lee SH, Lee EJ, Kim TW. Topographic correlation between juxtapapillary choroidal thickness and microstructure of parapapillary atrophy. Ophthalmology. 2016;123:1965–73.

34. Mammo Z, Heisler M, Balaratnasingam C, Lee S, Yu DY, Mackenzie P, et al. Quantitative optical coherence tomography angiography of radial peripapillary capillaries in glaucoma, glaucoma suspect, and normal eyes. Am J Ophthalmol. 2016; 170:41–9.

35. Rao HL, Pradhan ZS, Weinreb RN, Reddy HB, Riyazuddin M, Dasari S, et al. Regional comparisons of optical coherence tomography angiography vessel density in primary open-angle glaucoma. Am J Ophthalmol. 2016;171:75–83.

36. Suh MH, Zangwill LM, Manalastas PI, Belghith A, Yarmohammadi A, Medeiros FA, et al. Optical coherence tomography angiography vessel density in glaucomatous eyes with focal lamina cribrosa defects. Ophthalmology. 2016;123:2309–17.

37. Lee EJ, Lee KM, Lee SH, Kim TW. OCT angiography of the peripapillary retina in primary open-angle glaucoma. Investig Ophthalmol Vis Sci. 2016;57:6265–70.

38. Zhang HR. Scanning electron-microscopic study of corrosion casts on retinal and choroidal angioarchitecture in man and animals. Prog Retinal Eye Res. 1994;13:243–70.

39. Yu DY, Cringle SJ. Oxygen distribution and consumption within the retina in vascularised and avascular retinas and in animal models of retinal disease. Prog Retin Eye Res. 2001;20:175–208.